Supplementary material

For

A turn-on 'green channel' Zn^{2+} sensor and the resulting zinc(II) complex as a 'red channel' HPO_4^{2-} ion sensor: a new approach †

Somenath Lohar,[a] Siddhartha Pal,[a] Manjira Mukherjee,[a] Abhishek Maji,[a] Nicola Demitri[b] and Pabitra Chattopadhyay*,[a]

[a]*Department of Chemistry, Burdwan University, Golapbag, Burdwan-713104, West Bengal, India*

[b]*Elettra – Sincrotrone Trieste, S.S. 14 Km 163.5 in Area Science Park, 34149 Basovizza – Trieste, Italy*

CONTENTS

14. **Fig. S14.** plot for fluorescence intensity vs. concentration of HPO_4^{2-} ions

15. **Fig. S15.** Time-dependence profile for fluorescent detection of HPO_4^{2-} ions

16. **Fig. S16.** Selectivity study of dinuclear zinc(II) complex(**1**) and Change of relative fluorescence intensity profile of **1** in presence of different anions.

17. **Fig. S17.** Calibration curve for the nanomolar range, for calculating the LOD of HPO_4^{2-} ions by dinuclear zinc(II) complex(**1**) in DMSO solution.

18. **Fig. S18.** Solvent effect of **L′H, L′H**+Zn^{2+} ion(**1**) and 1+HPO_4^{2-} ions

19. **Fig. S19.** UV-vis and Fluorescence spectra of **L′H, L′H+base, 1**, **1+HPO_4^{2-}** in DMSO solution at 25 °C.

20. **Fig. S20.** Mass spectrum of the dinuclear zinc(II) complex (**1**) in presence of of HPO_4^{2-} ion.

21. **Fig. S21.** ^{1}H NMR spectrum of the dinuclear zinc(II) complex (**1**) in presence of of HPO_4^{2-} ion.

16. **Table S1** Crystal data and details of refinements for dinuclear zinc(II) complex (**1**).

17. **Table S2** Selected bond distances (Å) and bond angles (°) for dinuclear zinc(II) complex (**1**).

18. **Table S3** Life time detail of **1** in absence and presence of HPO_4^{2-} ions

Materials and physical measurements

2,6-diformyl-4-methyl-phenol was synthesized following the literature procedure[1], *3-amino-5-phenylpyrazole*, zinc acetate dihydrate, all other salts were purchased from Sigma-Aldrich and were used without further purification. Electrospray ionization Mass spectra (ESI-MS) were determined on a Qtof Micro YA263 and Thermochem Exactive Plus mass spectrometer. Microanalysis (C, H, and N) was performed using a Perkin-Elmer 2400 elemental analyzer. Fourier transform infrared (FTIR) spectra was done as KBr pellets using a Prestige-21 FTIR spectrophotometers. ^{1}H NMR and ^{13}C NMR spectra were recorded on a JEOL 400 and Bruker Avance DPX 400 MHz spectrometer instrument respectively in DMSO-d_6 using TMS as an internal standard. Melting points were determined on a hot-plate melting point apparatus in an open-mouth capillary and are uncorrected. Electronic spectra were recorded with a Shimadzu UV-1800 spectrophotometer. Fluorescence spectra measurements were performed on a Hitachi F-4500 spectrofluorimeter.

The spectroscopic studies of **L′H** were recorded in DMSO. For the selectivity study of **L′H**, stock solutions (~ 10^{-2} M) of different metal ions were prepared taking nitrate salts of Na^+, K^+, Cu^{2+}, Cr^{3+}, Al^{3+}, Pb^{2+}, Cd^{2+}, Ag^+; acetate salt of Mn^{2+}, Zn^{2+}; chloride salts of Co^{2+}, Ni^{2+}, Ca^{2+}, Hg^{2+}, Mg^{2+}, Fe^{3+}, and Fe^{2+} sulphate. In this selectivity study, the amount of the metal ions was fifty times greater than

that of the probe used. Fluorescence titration with zinc acetate was performed in DMSO varying the metal concentration from 0 to 15 μM and the concentration of **L′H** was fixed at 5 μM. Tetrabutylammonium salts of dihydrogen phosphate, acetate, halides (F^-, Cl^-, Br^-, I^-); and sodium/potassium salts of arsenate, arsenite, bicarbonate, nitrate, chlorate, monohydrogen phosphate, phosphate, azide, cyanide, thiocyanate, sulphate and pyrophosphate etc were used for the selectivity study of the receptor towards different anions. Fluorescence titration with HPO_4^{2-} was carried out adding the anion concentration upto 3equivalent [concentration of dinuclear zinc(II) complex (**1**) was fixed at 25 μM].

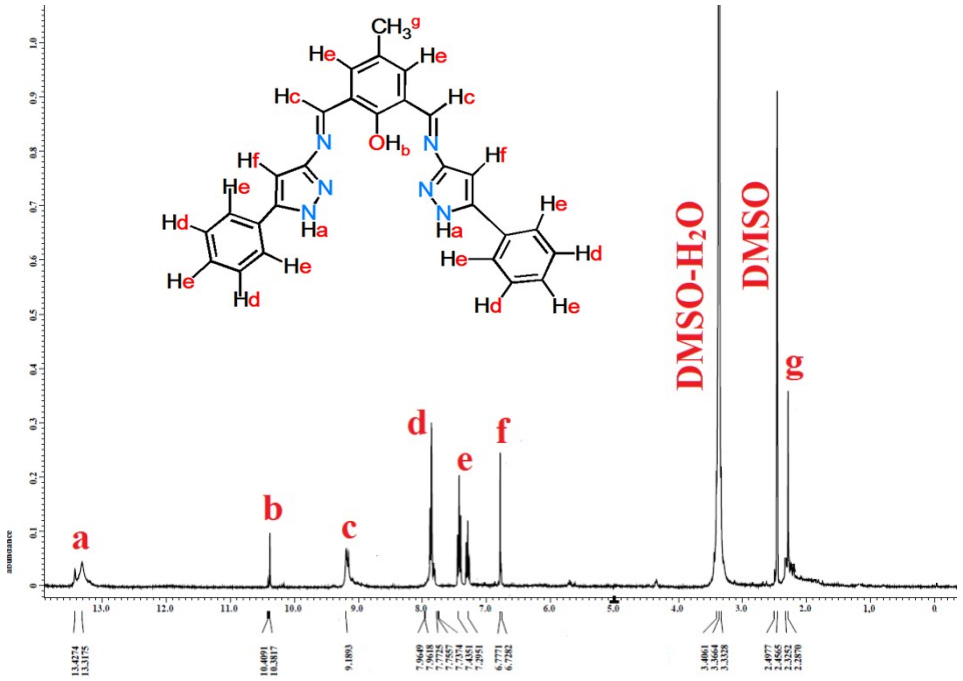

Fig. S1. ^{1}H NMR spectrum of **L′H** in DMSO-d_6

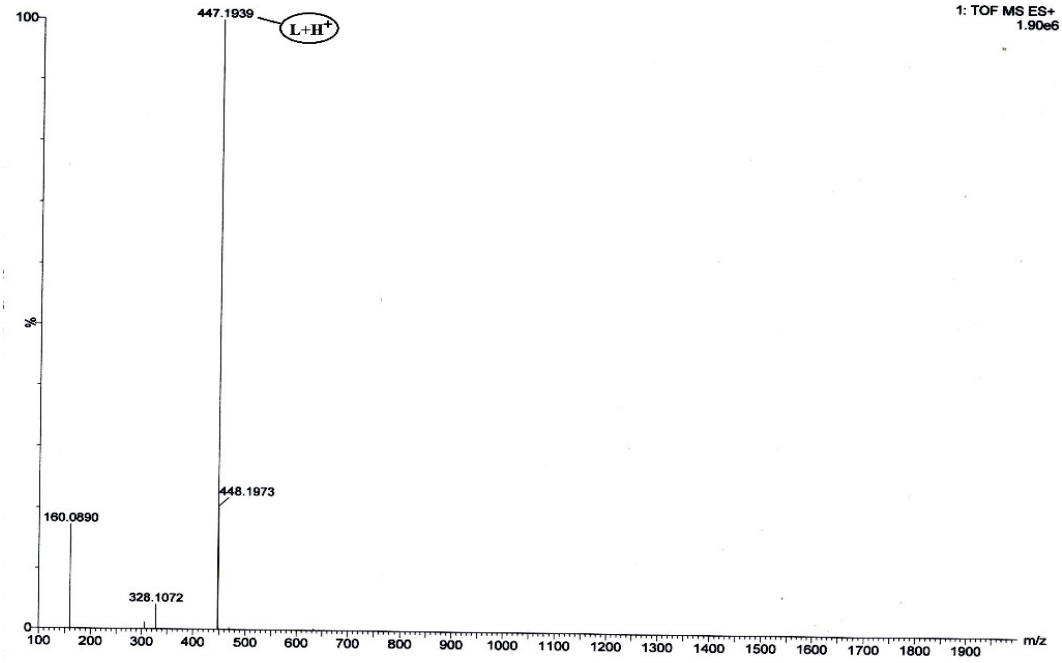

Fig.S2. Mass spectrum of **L′H**

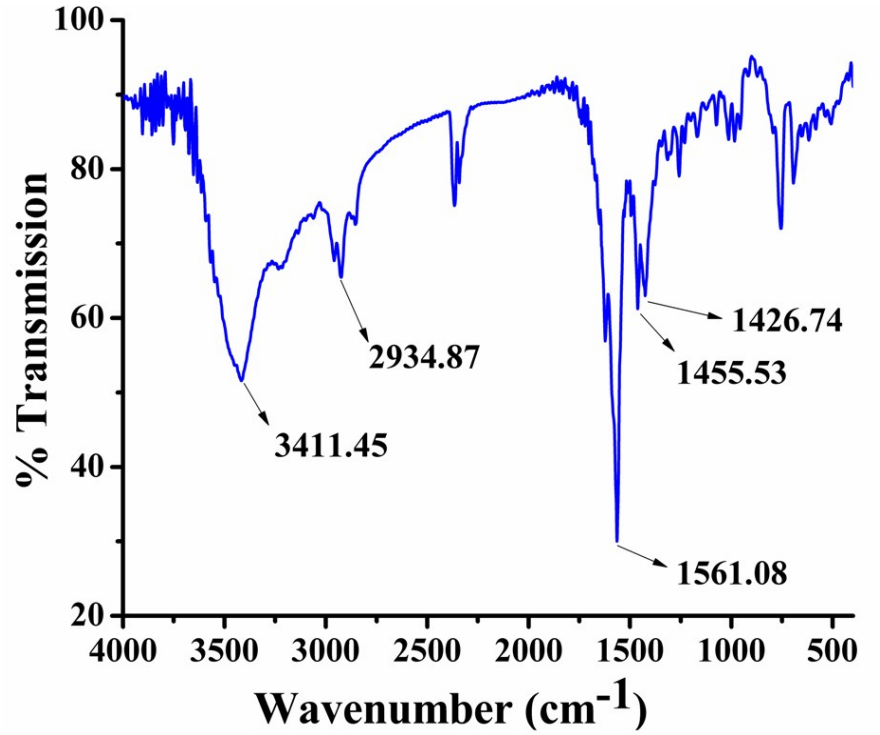

Fig. S3. IR spectrum of **L′H**

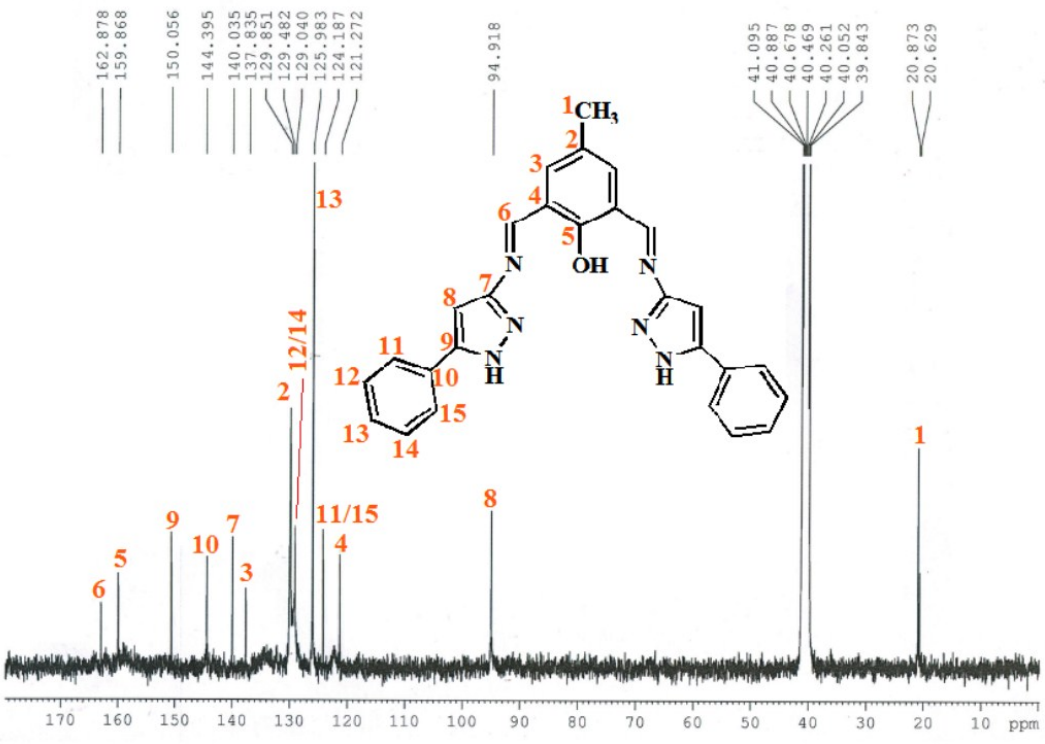

Fig. S4. ^{13}C NMR spectrum of **L′H** in DMSO-d_6

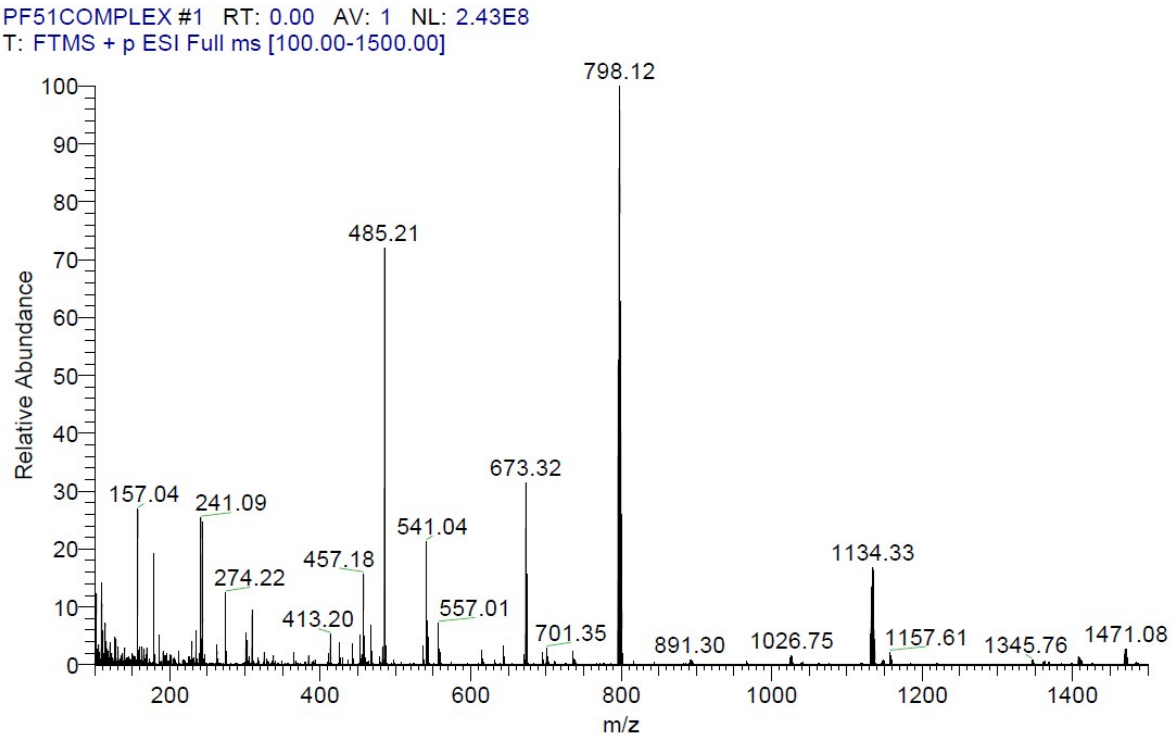

Fig.S5. Mass spectrum of dinuclear zinc(II) complex (**1**)

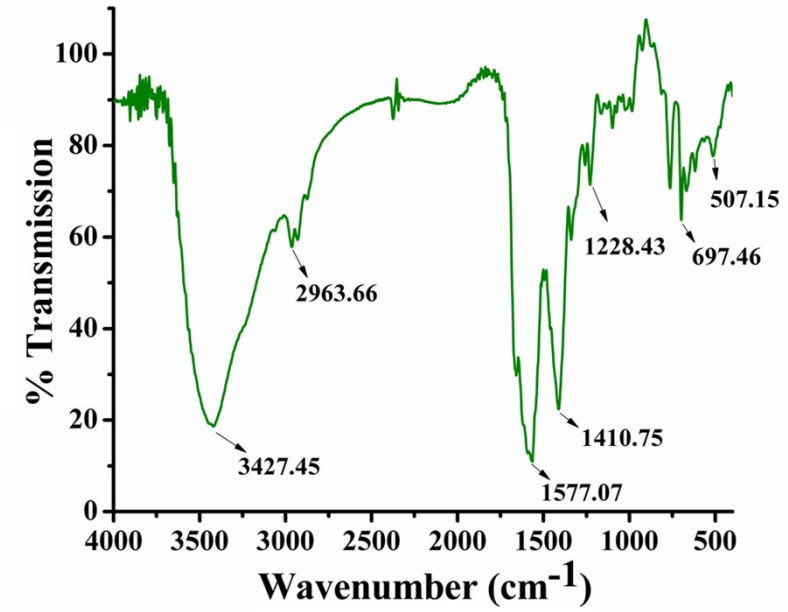

Fig. S6. IR spectrum of dinuclear zinc(II) complex (**1**)

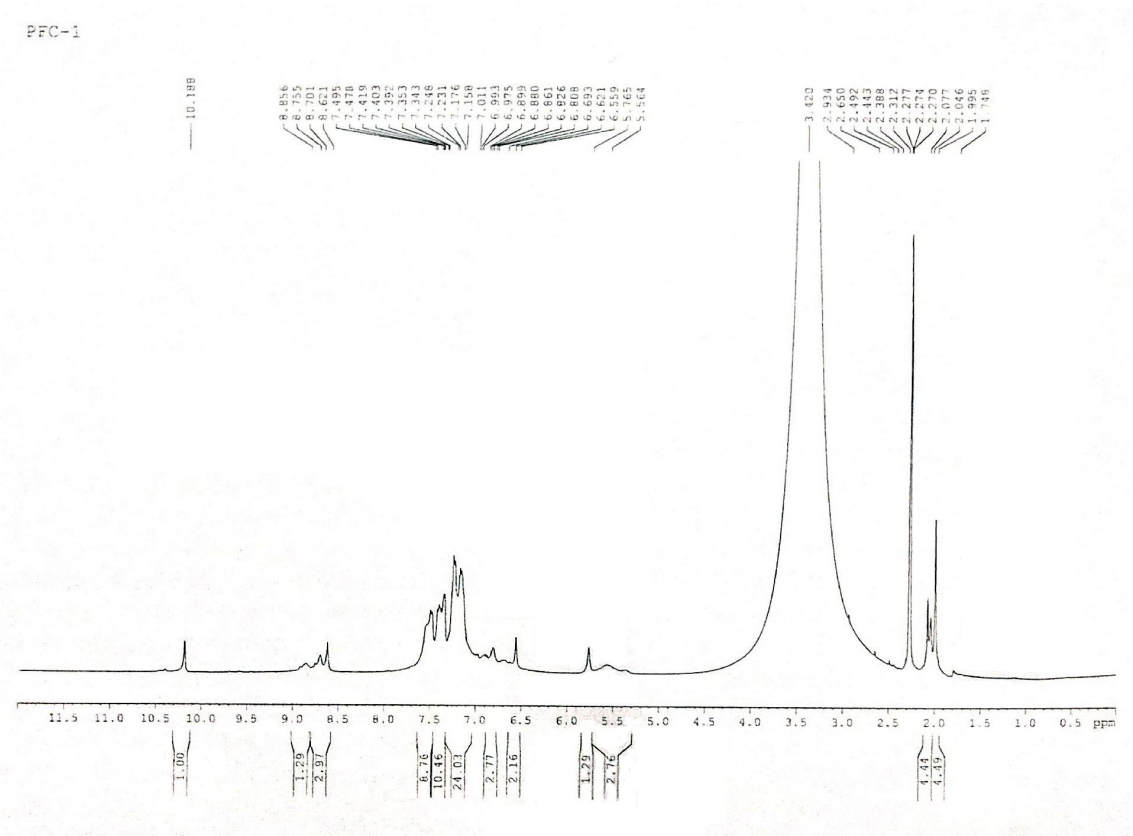

Fig. S7. ^{1}H NMR spectrum of dinuclear zinc(II) complex (**1**) in DMSO-d_6

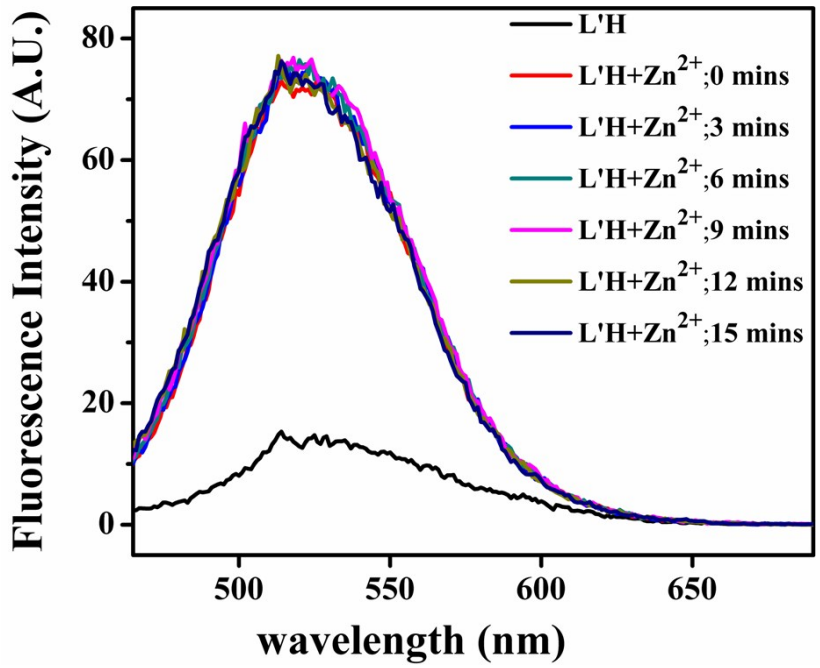

Fig. S8. Time-dependence profile for fluorescent detection of Zn^{2+} ion

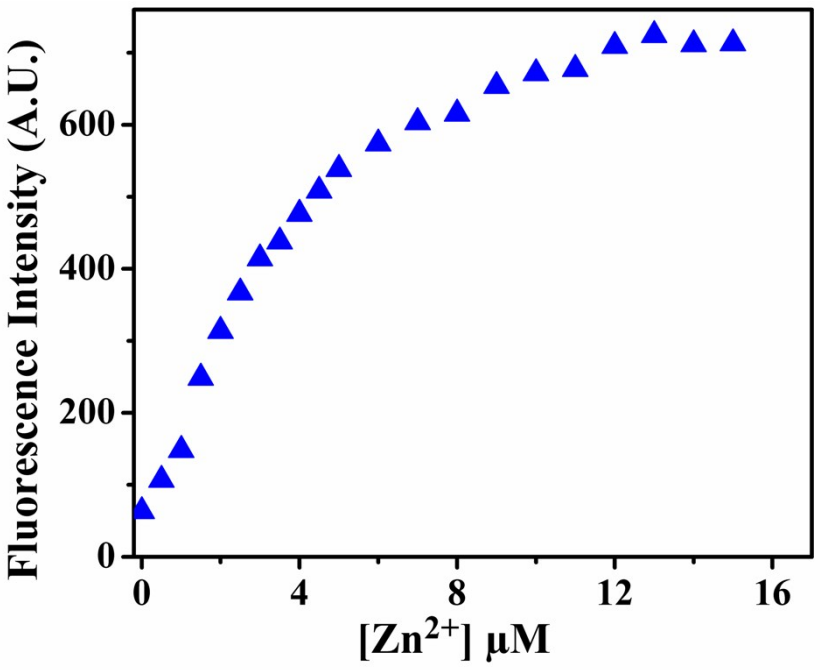

Fig. S9. Plot for fluorescence intensity vs. concentration of Zn^{2+} ions

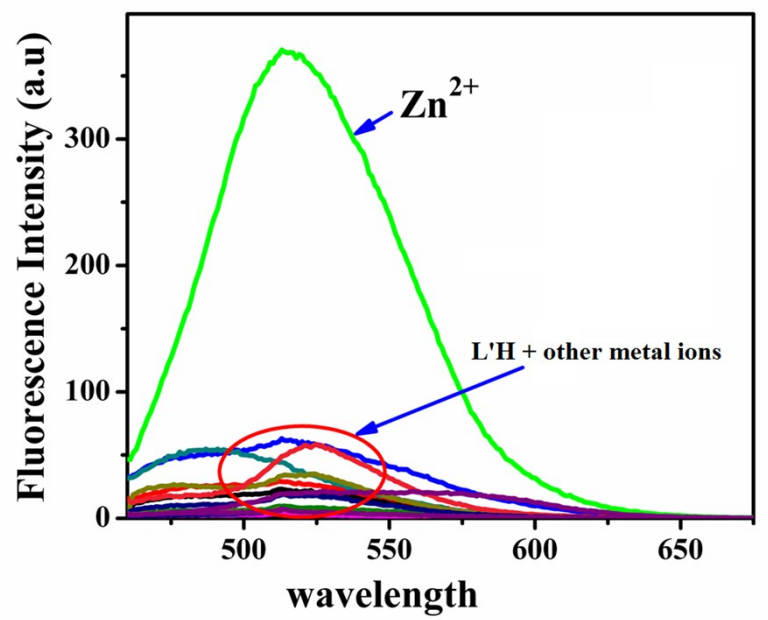

Fig. S10. Selectivity study of **L′H** in presence of different metal ions.

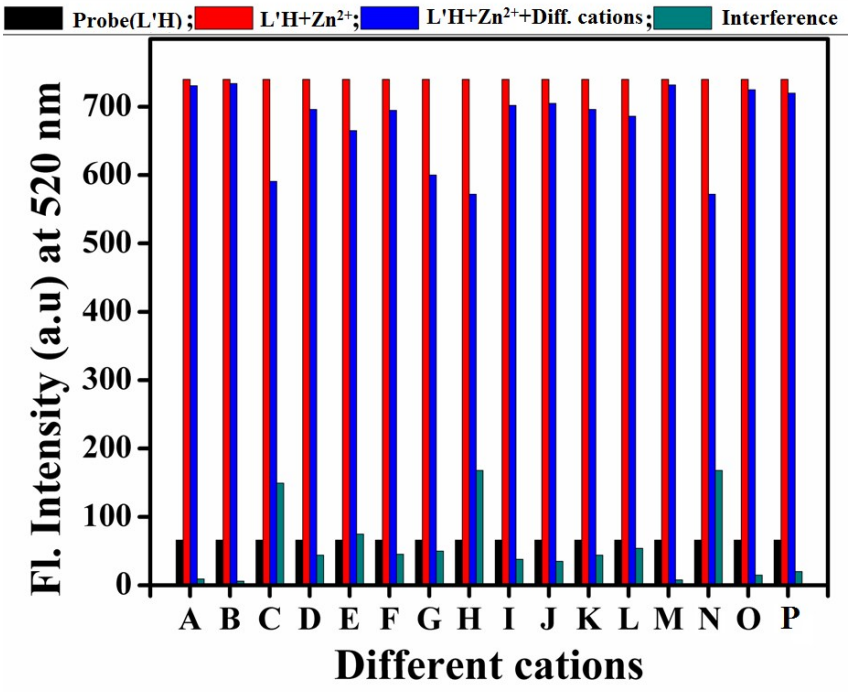

Fig. S11. Change of relative fluorescence intensity profile of **L′H** in presence of different cations in DMSO solution (A) Ca^{2+}, (B) Mg^{2+}, (C) Al^{3+}, (D) Mn^{2+}, (E) Co^{2+}, (F) Pb^{2+}, (G) Cr^{3+}, (H) Ni^{2+}, (I) Cd^{2+}, (J) Fe^{2+}, (K) Fe^{3+}, (L) Hg^{2+}, (M) Cu^{2+}, (N) Na^{+}, (O) K^{+}, (P) Ag^{+}.

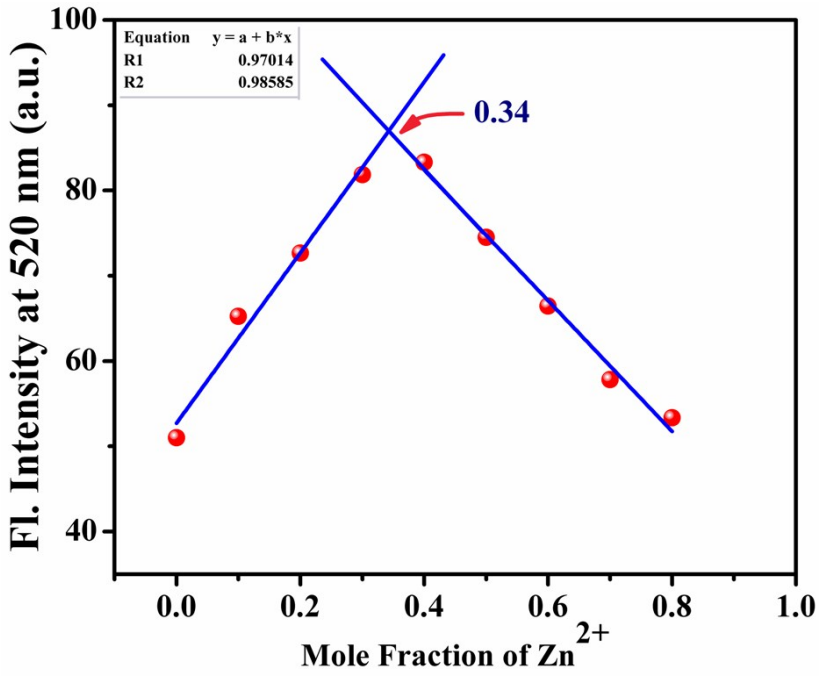

Fig. S12. Job's plot of **L′H** showing 1:2 (Zn^{2+}: **L′H**) stoichiometry

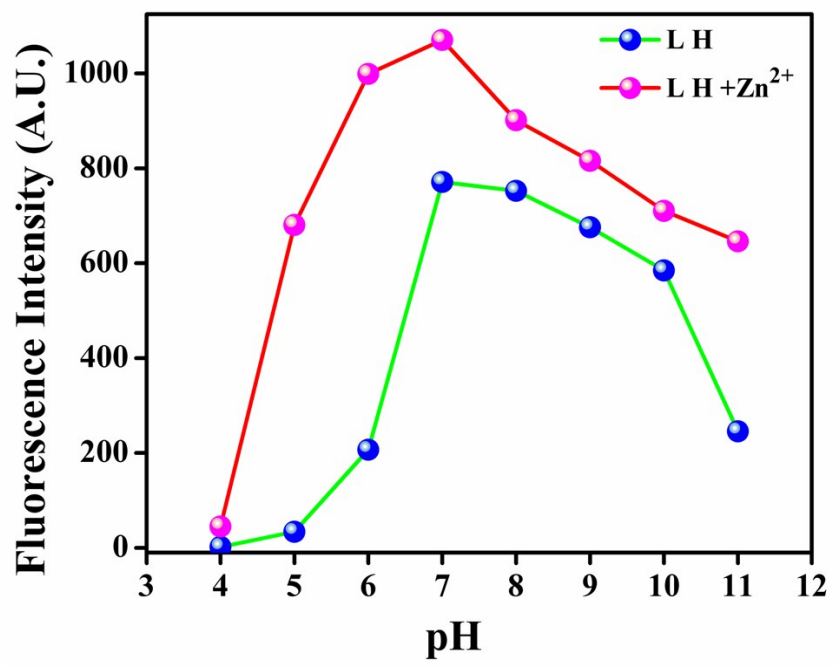

Fig. S13. The pH dependence of fluorescence spectra of **L′H** in absence and presence of Zn^{2+}

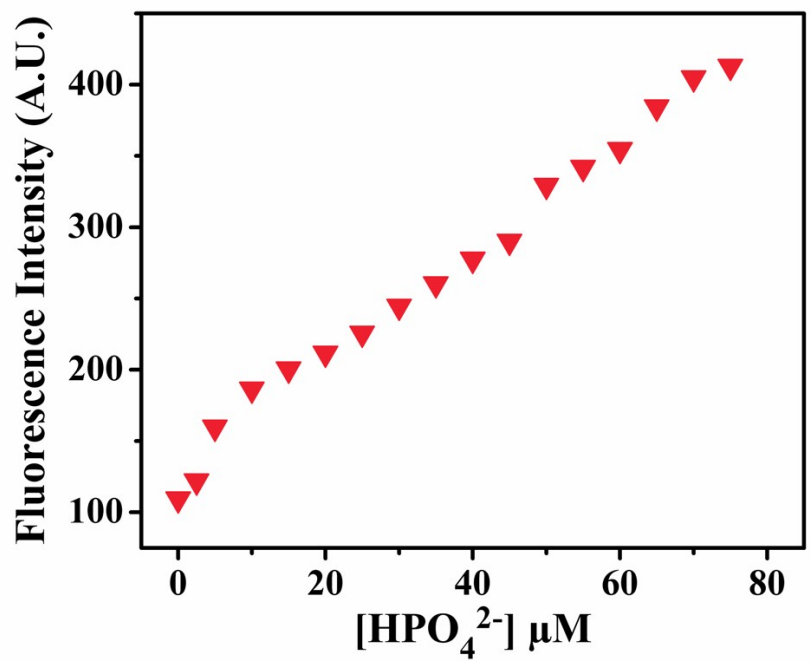

Fig. S14. Plot for fluorescence intensity vs. concentration of HPO_4^{2-} ions

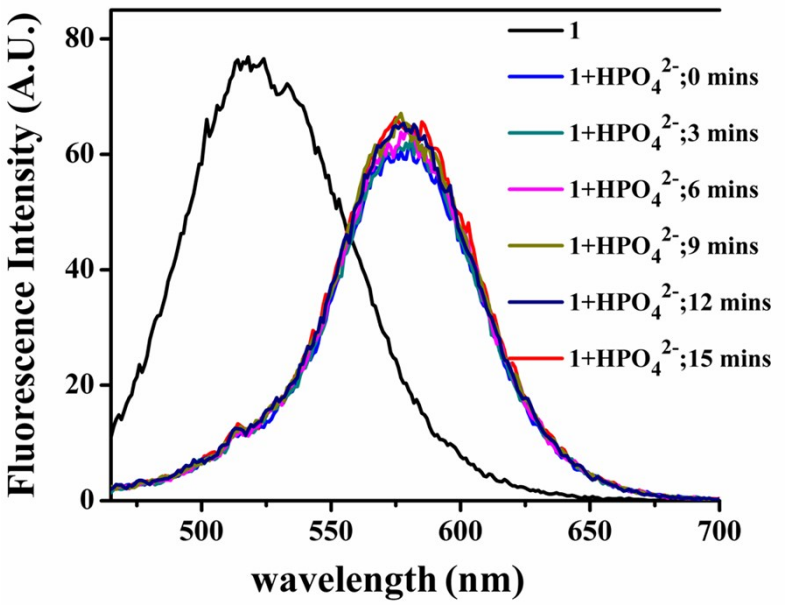

Fig. S15. Time-dependence profile for fluorescent detection of HPO_4^{2-} ions

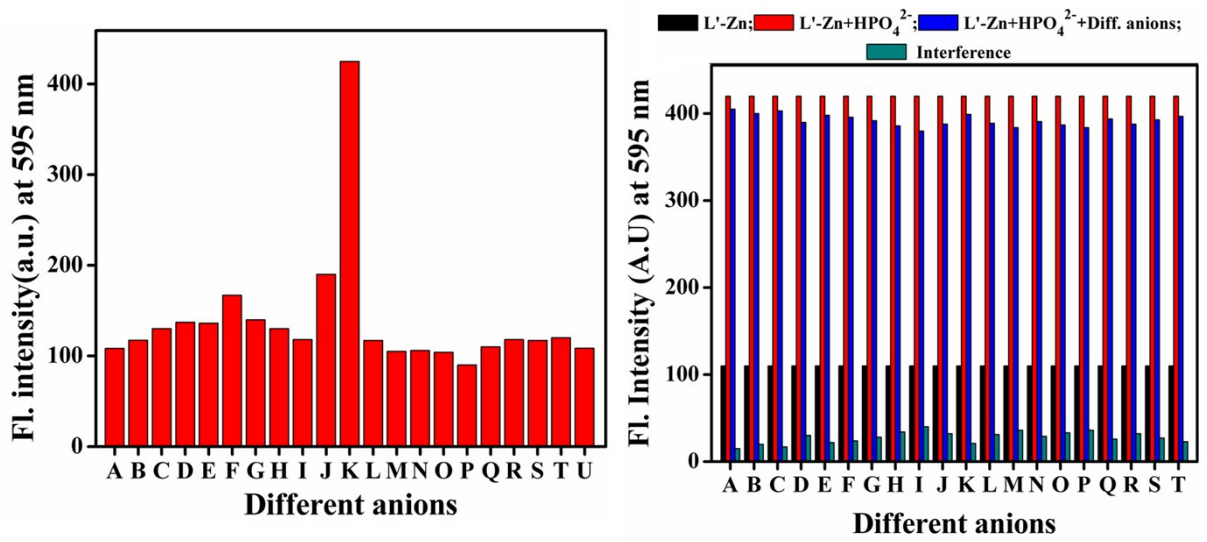

Fig. S16. Selectivity study of dinuclear zinc(II) complex(**1**) in presence of different metal ions[left] Change of relative fluorescence intensity profile of dinuclear zinc(II) complex (**1**) in presence of different anions in DMSO solution (A) SCN^-, (B) PO_4^{3-}, (C) MO_4^{2-} , (D) CN^-, (E) F^-, (F) Cl^-, (G) Br^-, (H) I^-, (I) $HAsO_4^{2-}$, (J) S^{2-}, (K) AcO^-, (L) $H_2AsO_4^-$, (M) SO_4^{2-}, (N) $H_2PO_4^-$, (O) HSO_4^-, (P) NO_3^-, (Q) CO_3^{2-}, (R) HCO_3^-, (S) ClO_4^- and (T) $P_2O_7^{4-}$ [right].

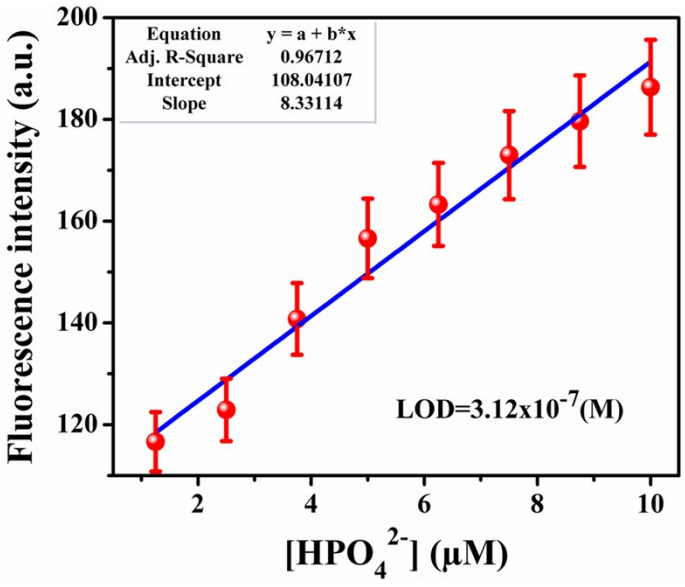

Fig. S17. Calibration curve for the nanomolar range, for calculating the LOD of HPO_4^{2-} ions by dinuclear zinc(II) complex (**1**) in DMSO solution.

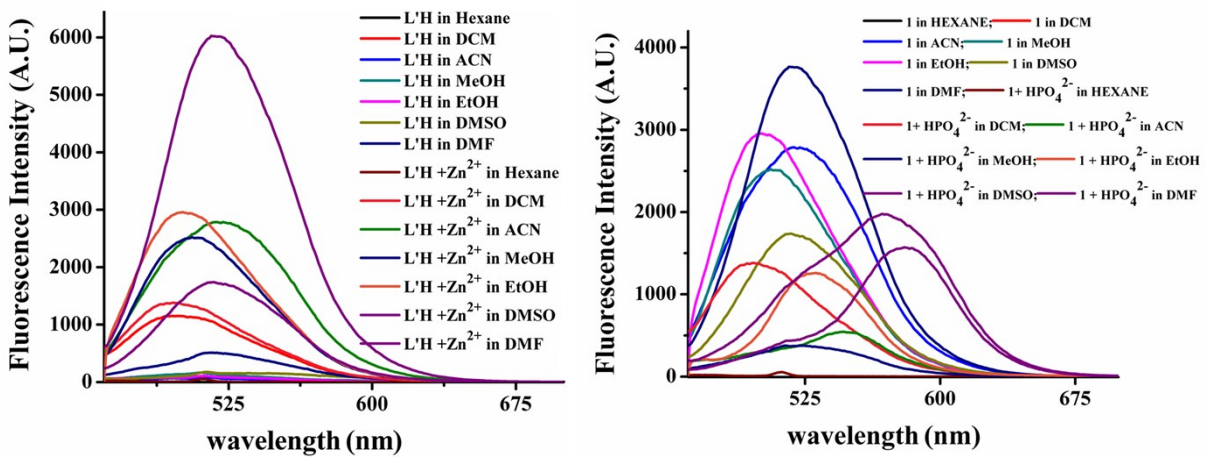

Fig. S18. Solvent effect of **L′H, L′H**+Zn^{2+} ion(**1**) and 1+HPO_4^{2-} ions

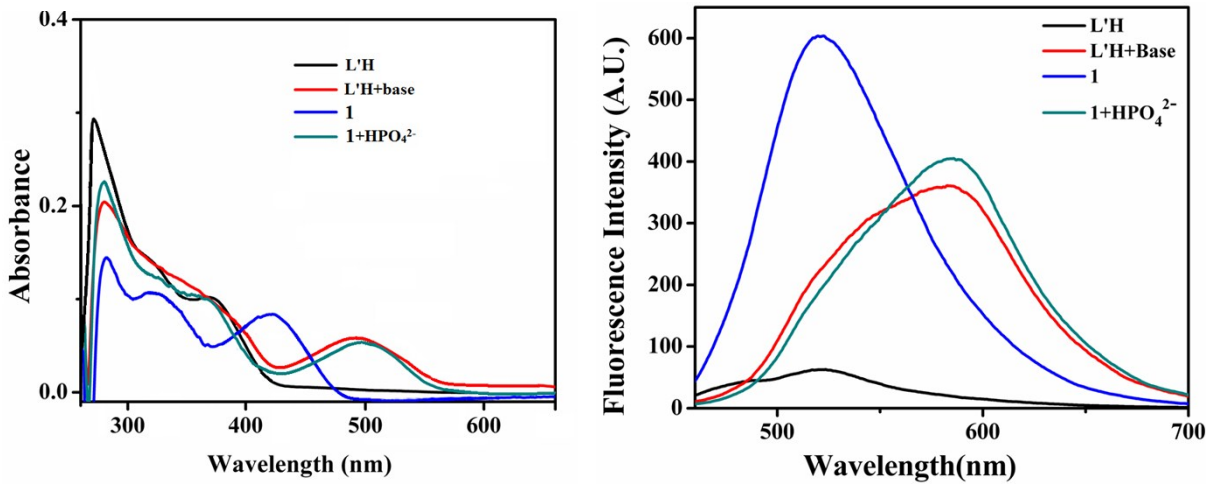

Fig. S19. UV-vis and Fluorescence spectra of **L′H, L′H +base, 1** and **1+HPO_4^{2-}** in DMSO at 25 °C

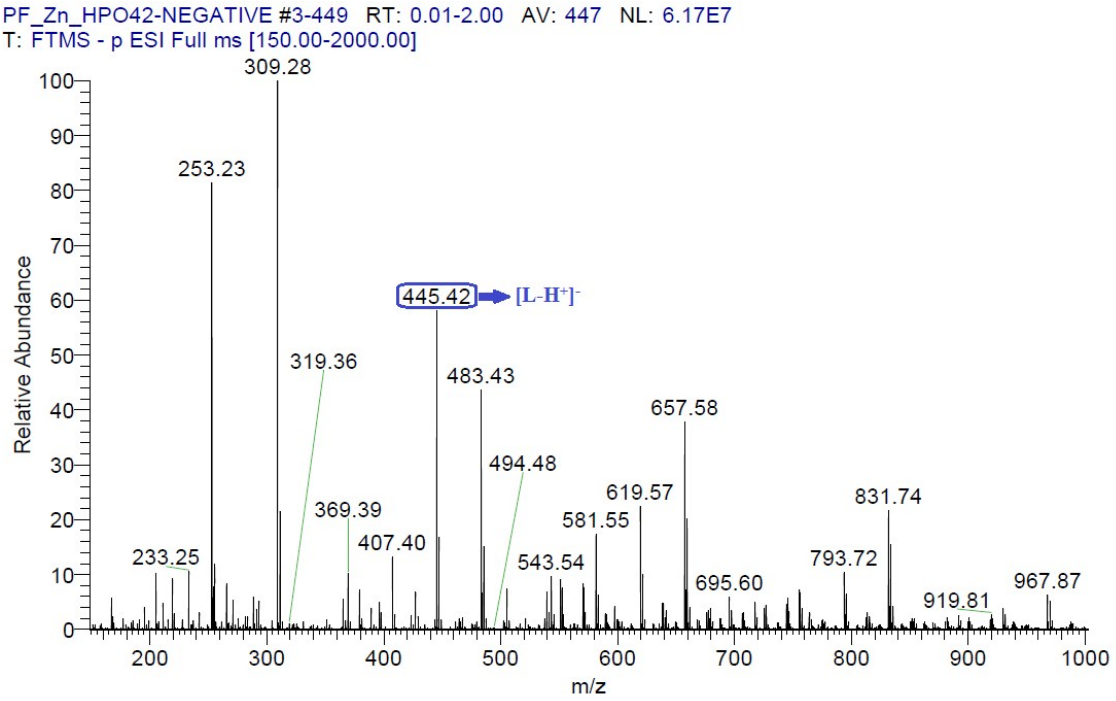

Fig. S20. Mass spectrum of dinuclear zinc(II) complex (**1**) in presence of HPO_4^{2-} ions

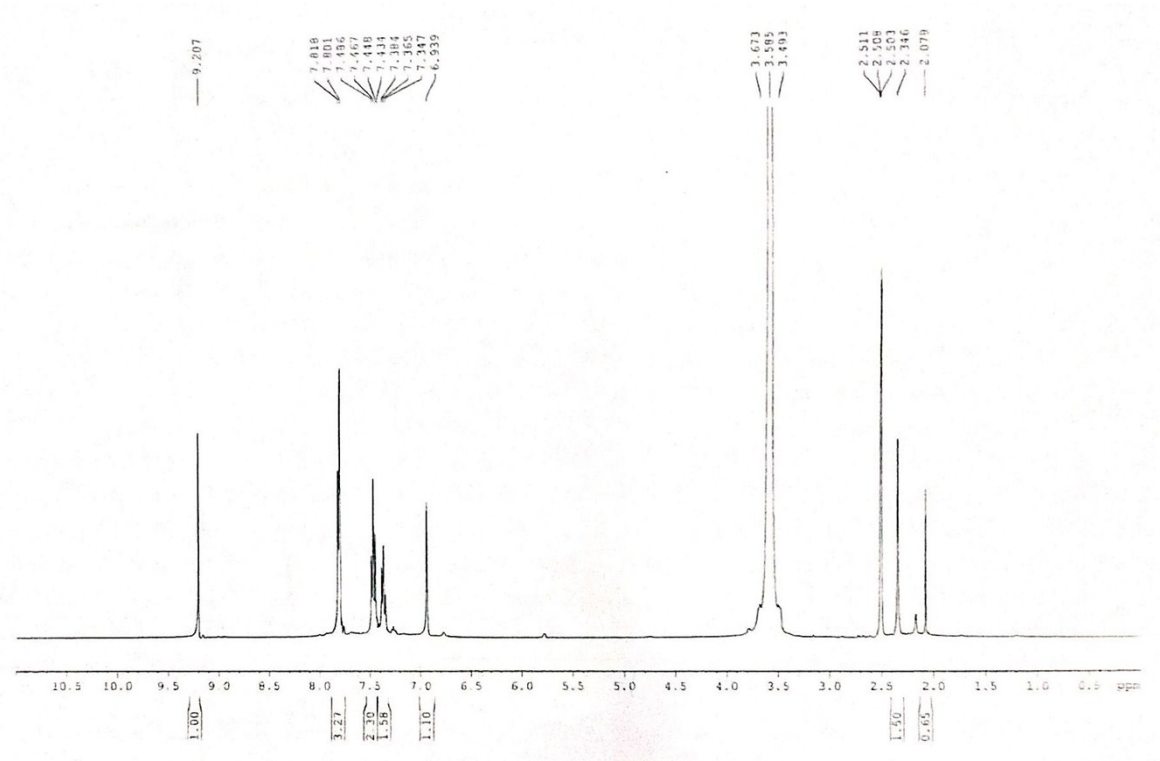

Fig. S21. ^1H NMR spectrum of the dinuclear zinc(II) complex (**1**) in presence of of HPO_4^{2-} ion in DMSO-d_6.

Table S1 Crystal data and details of refinements for dinuclear Zinc(II) complex (**1**).

Empirical Formula	$C_{90}H_{72}N_{18}O_7Zn_2$	ρ_{calc} (g/cm^3)	1.287
Formula Weight	1648.39	μ (mm^{-1})	0.565
Crystal system	monoclinic	F(000)	1708
Space group	*P* c	θ range (deg)	1.14 - 25.27°
a (Å)	18.413(4)	Reflections collected	28734
b (Å)	16.514(3)	Reflections independent	14884
c (Å)	14.665(3)	R_{int}	0.0899
β (deg)	107.49(3)	Goodness of fit	1.124
Volume (Å^3)	4253.2(16)	Final R indices [$I > 2\sigma(I)$]	R = 0.1063
Z	2		wR2 = 0.2630

Table S2 Selected bond distances (Å) and bond angles (°) for dinuclear Zinc(II) complex (**1**).

Bond lengths (Å)			
Zn(1)-O(1)	2.083(8)	Zn(1)-O(1w)	2.200(10)
Zn(1)-N(1)	2.109(12)	Zn(2)-O(3)	1.943(9)
Zn(1)-O(2)	2.113(9)	Zn(2)-O(4)	1.952(9)
Zn(1)-N(7)	2.123(11)	Zn(2)-N(13)	2.082(11)
Zn(1)-O(2w)	2.167(12)	Zn(2)-N(16)	2.097(10)
Bond angles (º)			
O(1)-Zn(1)-N(1)	83.4(4)	O(1)-Zn(1)-O(1w)	177.5(4)
O(1)-Zn(1)-O(2)	90.6(3)	N(1)-Zn(1)-O(1w)	95.3(4)
N(1)-Zn(1)-O(2)	90.1(4)	O(2)-Zn(1)-O(1w)	91.5(4)
O(1)-Zn(1)-N(7)	90.2(4)	N(7)-Zn(1)-O(1w)	91.4(4)
N(1)-Zn(1)-N(7)	170.4(4)	O(2w)-Zn(1)-O(1w)	85.3(4)
O(2)-Zn(1)-N(7)	82.9(4)	O(3)-Zn(2)-O(4)	158.6(4)
O(1)-Zn(1)-O(2w)	92.5(4)	O(3)-Zn(2)-N(13)	92.6(4)
N(1)-Zn(1)-O(2w)	91.1(4)	O(4)-Zn(2)-N(13)	100.1(4)
O(2)-Zn(1)-O(2w)	176.8(4)	O(3)-Zn(2)-N(16)	100.7(4)
N(7)-Zn(1)-O(2w)	96.3(4)	O(4)-Zn(2)-N(16)	93.1(4)
		N(13)-Zn(2)-N(16)	103.2(4)

Table S3 Life time detail of dinuclear zinc(II) complex (**1**) in absence and presence of HPO_4^{2-} ions

	B_1	B_2	τ_1(ns)	τ_2(ns)	τ_{av}(ns)	χ^2	φ	K_r	K_{nr}	K_r / K_{nr}
1	94.05	5.95	0.487	1. 79	0.565	1.02	0.157	0.278	1. 49	0.186
1 + HPO_4^{2-} ions	100	-	2.25	-	2.25	1.00	0.342	0.152	0.292	0.52

References

[1] R.R. Gagne, C.L. Spiro, T.J. Smith, C.A. Hamann, W.R. Thies and A.K. Schiemke, *J. Am. Chem. Soc*., 1981, **103**, 4073.